COBEM 2023 27TH INTERNATIONAL CONGRESS OF MECHANICAL ENGENEERING

ABCM Brazilian Society of Mechanical Sciences and Engineering
27th ABCM International Congress of Mechanical Engineering
December 04-08, 2023, Florianópolis-SC, Brazil

COB-2023-0791
COMPARING ANALYTICAL AND NUMERICAL SOLUTIONS FOR FLUID STRUCTURE PROBLEMS WITH FREE SURFACE CONDITIONS: A STUDY ON TUNED LIQUID DAMPERS AND TUNED LIQUID COLUMN DAMPERS

Pedro Falcomer Pontes Viégas
University of Brasilia,Faculdade do Gama Campus, 72444-240, Gama, Brazil

Marcus Vinicius Girão de Morais
University of Brasília, Darcy Ribeiro Campus, Asa Norte, Brasília, DF 70910-900, Brazil.
pedrofalcomerpv@gmail.com, mvmorais@unb.br

Agnaldo Antônio Moreira Teodoro da Silva
Raul Dario Durand Farfan
University of Brasília, Darcy Ribeiro Campus, Asa Norte, Brasília, DF 70910-900, Brazil.
professoragnaldoantonio@gmail.com; durand@unb.br

Abstract. *This paper presents a finite element analysis of sloshing in 3D water tanks using a pressure based Eulerian approach. The fluid domain is discretized by isoperimetric elements (FLUID220) that exhibit a quadratic pressure behaviour. Used for modelling the fluid domain. Three examples (a rectangular cavity, a square tuned liquid column damper – TLCD - and a bi-directional tuned liquid multicolumn damper – TMLCD-) were modelled with rigid contours and a free surface to study uncoupled liquid reservoirs. Free vibration and harmonic analysis were performed to determine dynamic parameters of the three cases. For the rectangular cavity the numerical results are compared to analytical solutions, and previous numerical and experimental studies. The numerical solutions present acceptable relative error (inferior to 0.2% relative error) when compared to analytical solutions. For the TLCD example, the numerical results were validated using experimental results and previous numerical studies, presenting acceptable errors (6% relative error). For the third case the modal results were compared to the analytic solution and previous works returning an error of 2,75 and 3,14% relative to the experimental values and the harmonic analysis presented a reduction of 44,88% in the amplitude of displacement of the system, thus validating this approach of analysis in the development of this kind of device.*

Keywords: *Sloshing, TLCD, Fluid-Structure Interaction, Acoustic Finite Element Modelling, Structural Vibration*

1. INTRODUCTION

Tuned liquid column damper (TLCD) is a kind of passive damper device used to control structural vibration in tall buildings, wind turbines and ships. These passive devices are characterized as fluid-structure problems. Free surface problems can be modelled as TLD and TLCD to describe the behavior in top of tall and slender structures.

TLCDs were first proposed in tall buildings by Sakai *et al.* (1989). In the literature, this passive device is attractive for wind turbines due to its relatively low cost and good efficiency at low frequencies (Colwell and Basu 2009). Yalla and Kareem (2000) proposed an approximate optimized solution for the TLCD head loss gain for a white noise spectrum. Alkmin, Fabro, and Morais (2018) optimized linearized TLCD parameters for a classic wind spectrum. Martins Morais and Avila (2019) experimentally showed the reduction of vibration of a TLCD in a reduced linear structure. There is also a small difference between theoretical frequencies and experimental results (Alkmim et al. 2018; Martins et al. 2019).

This study aims to compare analytical and numerical solutions of fluid-structure problems with free surface conditions, such as Tuned Liquid Damper (TLD) and Tuned Liquid Column Damper (TLCD). The fluid domain is discretized by isoperimetric elements (FLUID220) that exhibit a quadratic pressure behaviour. Used for modelling the fluid domain. Three problems were presented: (a) a rectangular water tank, (b) a U-shaped tube filled with a liquid and (c) a multiple column damper. For the rectangular cavity the numerical results are compared to analytical solutions, and previous numerical and experimental studies. The numerical solutions present acceptable relative error (inferior to 0.2% relative error) when compared to analytical solutions. For the TLCD example, the numerical results were validated using experimental results and previous numerical studies, presenting acceptable errors (6% relative error). For the third case the results were compared to the analytic solution and previous works returning a relative error of 3,27%. The present numerical implementation presents a good agreement with the analytical solution and experimental results.

2. WAVE EQUATION

For the discretization of the acoustic wave equation, the following assumptions are made:

i. The fluid is compressible and homogeneous.
ii. The fluid is inviscid and irrotational.
iii. There is no mean flow of the fluid.
iv. The acoustic pressure is defined as the pressure fluctuation about the mean.
v. The change in density is small compared to the mean density.
vi. The pressure and density can vary across elements.

In a compressible fluid, acoustic waves are described as pressure fluctuations, meaning they have infinitesimal amplitudes. According to assumptions (i), (iv), and (v), the mass density, pressure and velocity are written as the sum of the mean values and a fluctuation, as shown by the equation.

$$\rho = \rho' + \rho_0 \qquad (\rho' \ll \rho_0) \tag{1}$$

$$p = p' + p_0 \qquad (p' \ll p_0) \tag{2}$$

$$u = u' + u_0 \qquad (u' \ll u_0) \tag{3}$$

where: ρ is the density, ρ_0 is the average density and ρ′ is the density fluctuation. As the flow is zero the average flow $u = 0$ so the average velocity $u = u'$. For the description of the wave equation, a combination of Navier Stokes, continuity and state equations are used. These equations are presented below:

$$\frac{d\rho}{dt} + \nabla(\rho u) = 0 \tag{4}$$

$$\rho\left(\frac{d\rho}{dt} + u\nabla u\right) = -\nabla p + \mu\nabla^2 u + \frac{1}{3}\mu\nabla(\nabla * u) + \rho g \tag{5}$$

$$p' = c^2\rho \tag{6}$$

where: $c = \sqrt{k/\rho_o}$ is the velocity of propagation of sound in the fluid, K is the bulk modulus of the fluid and μ is the viscosity coefficient of the fluid.

Applying the divergent properties in the continuity equation and applying the density and velocity equations in the continuity equation results in

$$\frac{d(\rho' + \rho_0)}{dt} + (\rho' + \rho_0)\,\nabla \cdot u' + u'\nabla(\rho' + \rho_0) = 0 \tag{7}$$

The specific mass being independent of time in the first term and the third term of much lower order, the equation is rewritten in the form

$$\frac{d\rho'}{dt} + \rho_0\nabla \cdot u' = 0 \tag{8}$$

Starting with the Navier-Stokes equation, the fluid is considered inviscid, in this way

$$\rho\left(\frac{du}{dt} + u\nabla u\right) = -\nabla p + \rho g \tag{9}$$

As in this case there is no acoustic excitation, we have:

$$g\rho_0 = \nabla p_0 \tag{10}$$

Applying the pressure equation and the gradient properties results in the form:

$$\nabla p = \nabla p_0 + \nabla p' = g\rho_0 + \nabla p' \tag{11}$$

So, the continuity equation becomes:

$$\left(\frac{du'}{dt} + u\nabla u\right) = -\nabla p \tag{12}$$

where the nonlinear velocity term has negligible dimension and is rewritten as follows:

$$\rho\frac{du'}{dt} + \nabla p = 0 \tag{13}$$

Applying the divergence and deriving the continuity equation we obtain the wave equation

$$\frac{d^2\rho'}{dt^2} - \nabla^2 p' = 0 \tag{14}$$

or in linearized form:

$$\frac{1}{C^2}\frac{d^2p'}{dt^2} - \nabla^2 p' = 0 \tag{15}$$

considering the harmonic variation of the pressure

$$p = \underline{p}e^{-i\omega t} \tag{16}$$

$$\omega = 2\pi f \tag{17}$$

where $\underline{p}$ stands for the pressure amplitude, f for pressure oscillation frequency, and ω for angular frequency. By differentiating twice, the pressure equation and substituting it into the prior wave equation, the Helmholtz equation is obtained.

$$\frac{\omega^2}{C^2}\frac{d^2\underline{p}}{dt^2} + \nabla^2 p' = 0 \tag{18}$$

or in linearized form

$$\nabla^2\left(p + \frac{4}{3}\tau p'\right) = \frac{1}{C^2}\frac{d^2p}{dt^2} \tag{19}$$

where, velocity of sound $c = (K/\rho)^{0,5}$, in fluid medium, is function of density ρ and bulk modulus K, and dissipation constant $\tau = \mu/K$ is a function of viscosity and bulk modulus K, in this work τ is considered negligible.

2.1 Boundary conditions

To carry out this study, the fluid domain (Ω_F) is limited by the following boundary conditions: free surface (Γ_{SL}), rigid wall (Γ_{PR}) and fluid-structure interface (Γ_{FE}), given by:

- Free surface (Γ_{SL})

$$\frac{dp}{dZ} = -\frac{1}{g}\frac{d^2p}{dt^2} \tag{20}$$

- Rigid wall (Γ_{PR})

$$\frac{dp}{d\vec{n}} = \nabla p \cdot \vec{n} = 0 \tag{21}$$

- Fluid-Structure interface (Γ_{FE}), supposing ü=0

$$\frac{dp}{dn^{\rightarrow}} = \nabla p \cdot n^{\rightarrow} = -\rho_f \ddot{u} \tag{22}$$

where ρ_f, ü and g are the fluid density, the normal acceleration at the fluid-structure interface and the acceleration due to gravity.

3. PROBLEM DISCRETIZATION

The discretization of the wave equation, using the Galerkin method and an approximate function $\hat{p}$ that satisfies the boundary conditions, we have

$$\mathcal{R}(\hat{p}) = \nabla^2 \hat{p} - \frac{1}{c^2}\hat{p}'' \neq 0 \tag{23}$$

By the method of weighted residues, the integral of the residue $\mathcal{R}(\hat{p})$ with the approximation of $\hat{p}$ equals zero is expressed by:

$$\int_{\Omega f} \mathcal{R}(\hat{p})\, \hat{p} d\Omega = \int_{\Omega f} (\nabla^2 \hat{p} - \frac{1}{c^2}\hat{p}'')\, \hat{p} d\Omega = 0 \tag{24}$$

Applying Green's theorem and the boundary conditions results in the weak form of the sloshing equation

$$\int_{\Omega f} \nabla \hat{p} \nabla \hat{p} d\Omega + \oint_{\Gamma FE} \rho\, (\ddot{u} \cdot n)\, \hat{p} d\Gamma + \oint_{\Gamma SL} \frac{1}{g}\hat{p}''\, \hat{p} d\Gamma + \int_{\Omega f} \frac{1}{c^2}\hat{p}''\, \hat{p} d\Omega = 0 \tag{25}$$

4. NUMERICAL IMPLEMENTATION

The discretization of the wave equation, using the Galerkin method and an approximate function $\hat{p}$ that satisfies the boundary conditions, we have

The weak form shown in equation 25, was discretized using isoparametric finite elements. The element adopted was FLUID220, a tri-dimensional 20-node solid element with quadratic pressure behavior, for modeling the fluid medium, the fluid-structure interface and the free surface.

Assuming pressure in form of $\boldsymbol{p} \approx \hat{\boldsymbol{p}} \simeq \sum Ni\hat{p}i$, where $\hat{p}i$ are the nodal pressure of finite element at fluid domain, and Ni is spatial interpolating shape function, the discretized form of

$$K_f\, \hat{p} + \left\{\frac{1}{c^2} M_f + \frac{1}{g} M_{SL}\right\}\hat{p}'' = -\rho_f\, C_{FS}^T FS\, T\, u''_f \tag{26}$$

where, $\hat{\boldsymbol{p}}$ and $\hat{\boldsymbol{u}}$ are the nodal acoustic pressure in fluid domain Ωf and nodal solid acceleration in fluid-structure contour ΓFS, respectively. The matrix $\boldsymbol{K}f$ and $\boldsymbol{M}f$ are the acoustic 'stiffness' matrix and acoustic 'mass' matrix, respectively, given by:

$$\left(K_f\right)_{ijl} = \iiint_{-1}^{+1} \left(\frac{\partial N_i}{\partial \xi}\frac{\partial N_j}{\partial \xi}\frac{\partial N_l}{\partial \xi} + \frac{\partial N_i}{\partial \eta}\frac{\partial N_j}{\partial \eta}\frac{\partial N_l}{\partial \eta} + \frac{\partial N_i}{\partial \zeta}\frac{\partial N_j}{\partial \zeta}\frac{\partial N_l}{\partial \zeta}\right) |J|\, d\xi\, d\eta\, d\zeta \tag{27}$$

$$\left(M_f\right)_{ijl} = (1/c^2) \iiint_{-1}^{+1} N_i N_j N_l\, |J|\, d\xi\, d\eta\, d\zeta \tag{28}$$

where, $\boldsymbol{J}$ is the Jacobian matrix to transform global coordinate system (x, y, z) to natural coordinate system (ξ, η, ζ) ; $|J|$ = det $\boldsymbol{J}$; the Fluid 220 shape function $Ni = \xi i(2\xi i - 1)\eta i(2\eta i - 1)\zeta i(2\zeta i - 1)$; and $i \in [1,2,3\ldots,20]$.

The matrix $\boldsymbol{M}SL$ is the free-surface boundary condition, and $\boldsymbol{C}FS\ T$ is the fluid-structure coupling matrix using isoparametric L2 finite element, given by:

$$(MSL)_l = (1/g) \int_{-1}^{+1}\int_{-1}^{+1} N_l^T\, N_l\, |J|\, d\xi d\eta \tag{29}$$

$$(CFS\ T)_k = \rho_f \int_{-1}^{+1}\int_{-1}^{+1} N_k^T \cdot n\, N_k\, |J|\, d\xi d\zeta \tag{30}$$

where, $\boldsymbol{n}$ is the outwardly directed normal to the element surface along the interface. The numerical implementation was developed in Ansys Workbench, harmonic acoustics module (Ansys 2020R1)

5. NUMERICAL RESULTS

In this study, three cases are analyzed, a rectangular container (TLD), a U-shaped Column damper (TLCD) and a Multiple column damper (TLMCD), which were analyzed in terms of the modal response and the forced harmonic response, these results were then compared, with the analytic solutions, the literature and with simulations made in MATLAB and Ansys APDL in previous works. All cases are evaluated with the same parameters, density $\rho = 1000\ kg/m^3$, sound velocity $c = 1500\ m/s$, gravity acceleration, $g = 9{,}81\ m/s^2$ and the boundary conditions being composed of a rigid wall on all sides and free surface on the top faces.

5.1 Sloshing of rectangular container

For the first case, a rectangular container of dimensions $(L \times H) = (10 \times 10)\ [m^2]$ in x and y (negligible z dimension), Table 1 resume the natural frequencies simulated (for a converged mesh test) compared with previous studies and analytical data, done by expression:

$$\omega^2 = n\pi\ (g/L) \tanh[n\pi(H/L)] \tag{31}$$

where, n is the number of sloshing natural frequency.

Table 1. Convergence results for natural modes of vibration and frequencies of the rectangular container.

Frequency modes	Present study	MATLAB*	APDL*	Analytic.	Error P.S.	Error MATLAB [1]	Error APDL [1]
1	1,752	1,75	1,750	1,752	0,004%	0,129%	0,129%
2	2,483	2,48	2,450	2,478	0,181%	0,078%	1,133%
3	3,040	3,04	3,010	3,035	0,181%	0,165%	0,824%
4	3,511	3,52	3,450	3,505	0,183%	0,442%	1,556%

OBS: * da Silva and Morais (2018)

The results found show a good mesh convergence with the error relative lower than 0.2% as compared to analytical results. Figure 1 presents the first four sloshing modal shapes of rectangular container.

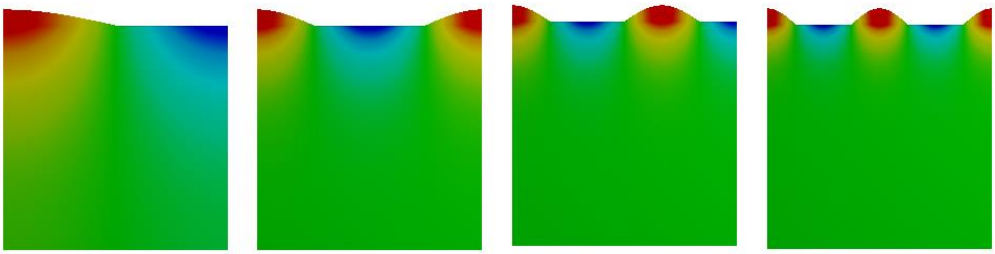

Figure 1. First four modes of resonance of the rectangular tank TLD.

After the modal analysis, the harmonic analysis, performed with the mass source excitation with a value of $1\ kg/mm^2$ applied on the left side, with positive X direction. The dynamic response of the fluid domain was evaluated at a point on the extreme left of the free surface. Figure 2 shows the frequency response function of measured point for a circular excitation frequency ω varying between 1.5 and 5 rad/s.

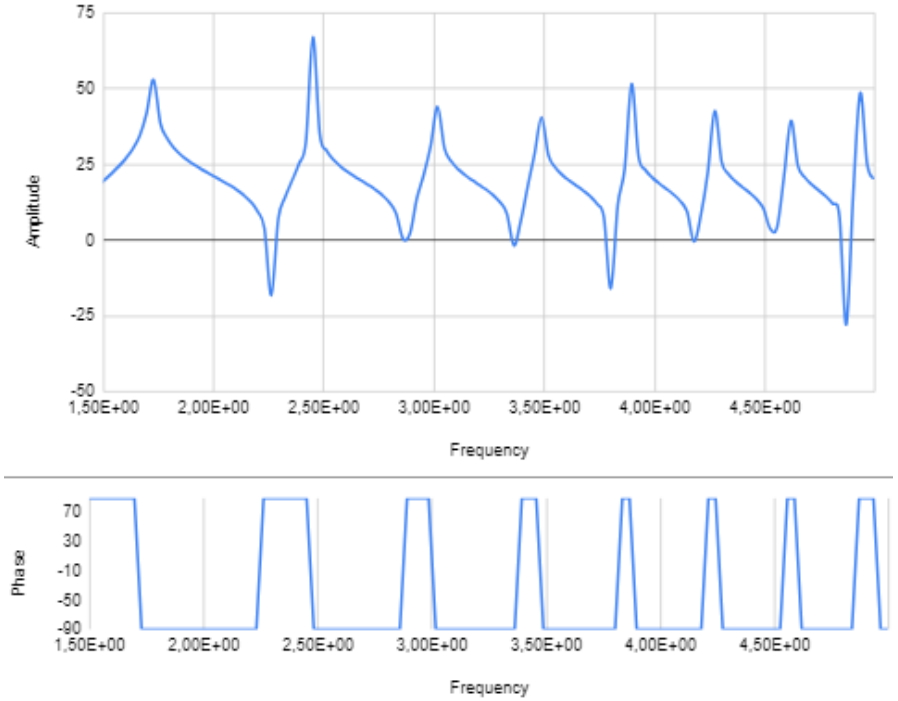

Figure 2. Frequency response function on the extreme left point of the free surface of the container.

5.2 Sloshing in TLCD

The analytical fundamental frequency of a TLCD is $\omega_1 = \sqrt{2g/L}$, where the total length $L = 2h_a + B$ of the TLCD. The others natural frequencies of TLCD $(n = 2,3,4, \dots)$ are similar to a rectangular container, replacing n by $n - 1$, so:

$$\omega_n^2 = \pi(n-1)(g/L')\tanh[\pi(n-1)(H'/L')], n = 2,3,4, \dots \quad (32)$$

where equivalent length $L' = 54mm$. $H' = h_a + (54/2)\ [mm]$ becomes the total height of a column and L its length.

The first modal frequencies for different column heights obtained (Figure 3) show reasonable concordance with the experimental results, 4,43% divergence and the maximum divergences of 8,6% with the analytical results. The higher discrepancies are attributed to the mesh refinement level.

Table 2 presents all the values for the first mode of resonance and the relative errors between when compared with the analytic and experimental values in comparison with previous studies.

Table 2. Convergence results for natural modes of vibration and frequencies of the TLCD

ha (mm)	Present study	MATLAB*	Analytic	Error MATLAB (%)	Error P.S. (%)	Experimental+	Error MATLAB (%)	Error P.S. (%)
35	1,42	1,39	1,31	6,11	8,60	1,38	0,72	3,09
45	1,37	1,34	1,27	5,51	8,19	1,33	0,75	3,31
55	1,33	1,29	1,23	4,88	7,82	1,27	1,57	4,43
65	1,28	1,25	1,19	5,04	7,73	1,23	1,63	4,23
75	1,24	1,21	1,16	4,31	7,05	1,20	0,83	3,48
85	1,21	1,18	1,13	4,42	6,65	1,17	0,85	3,01
95	1,17	1,14	1,10	3,64	6,47	1,15	-0,87	1,84
105	1,14	1,11	1,08	2,78	6,07	1,12	-0,89	1,80

OBS: * da Silva and Morais (2018), + Alckmin, Fabro and Morais (2018).

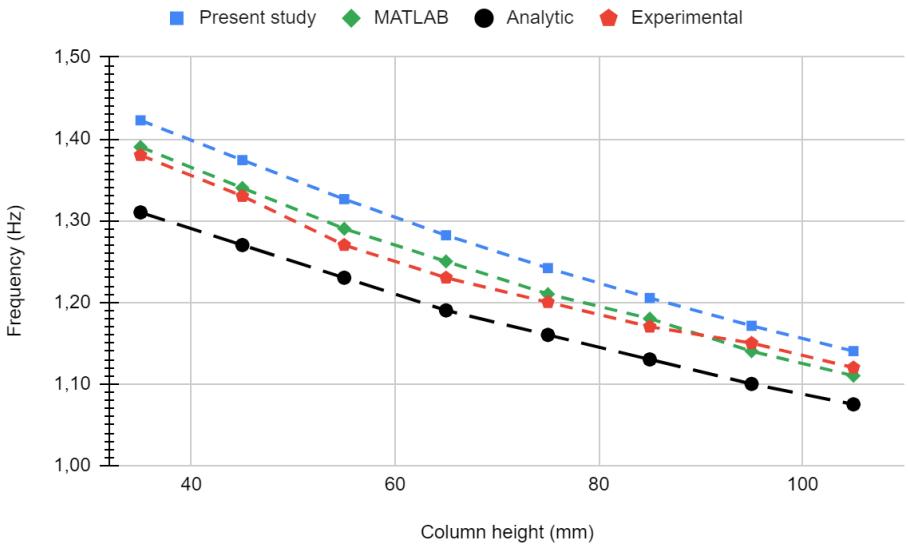

Figure 3. First mode natural frequency in hertz, with respect to column height from different studies.

Continuing the convergence analysis, Table 3 show compare the converged natural resonance frequencies founded in the present study for an uncoupled TLCD with $h_a = 105\ mm$ with previous studies (Alkmim et al. 2018; da Silva and Morais 2018) and analytical solution.

Table 3. Convergence results for natural modes of vibration and frequencies of the TLCD.

Frequency Modes	Present study	MATLAB*	Analytic	Error (P.S./Ana.)	Error (MATLAB/Ana.)
1	1,140	1,112	1,075	6,07%	3,44%
2	3,802	3,853	3,802	0,00%	1,34%
3	5,383	4,122	5,377	0,10%	23,34%
4	6,621	5,213	6,586	0,53%	20,84%

OBS: * da Silva and Morais (2018)

The results found for the natural frequencies in the X direction showed good convergence when compared to the analytically calculated values, with the highest deviation shown being 6,07% in the first mode.

Figure 4 shows the first four modal shapes of TLCD with $h_a = 105mm$.

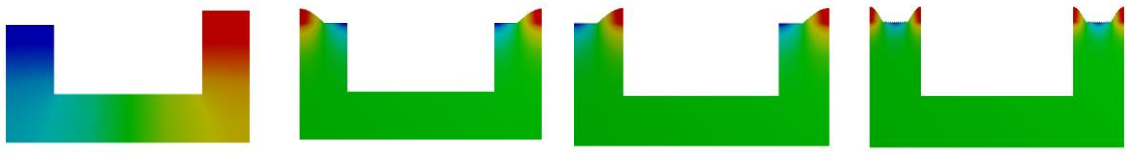

Figure 4. First four modal shapes the U-shaped TLCD with $h_a = 105mm$.

The harmonic analysis was performed with the same parameters as in the first case, mass source with a value of $1\ kg/mm^2$, applied to the left side, with a positive X direction, with the application point of the frequency response function being the extreme point left of the free surface. Figure 5 illustrates the frequency response function of this point with the frequency varying between 0 and 7 Hz.

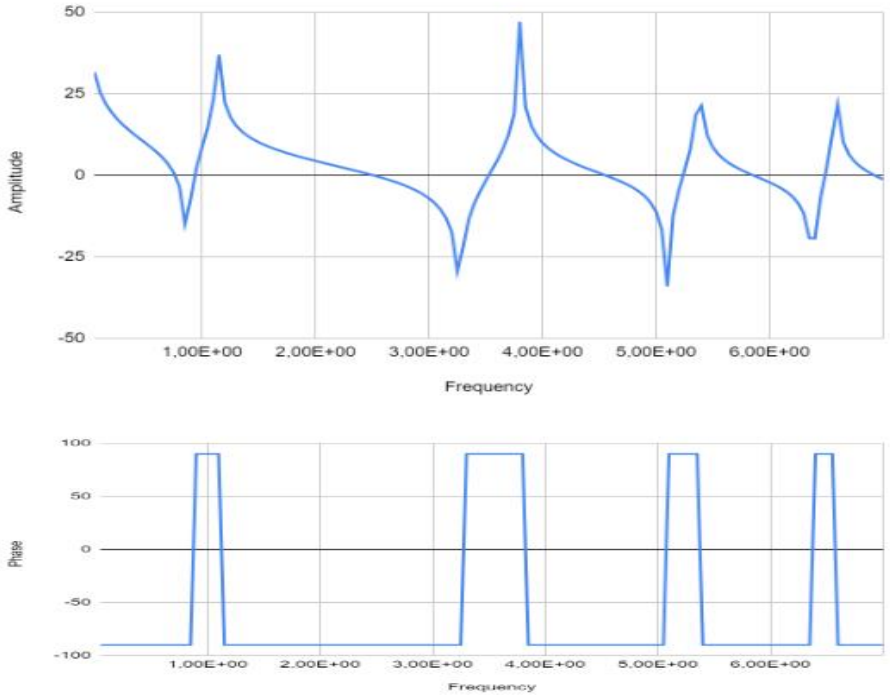

Figure 5. Frequency response function on the left most point of the free surface of the TLCD.

5.3 Sloshing of TMLCD

In the third case the selected tuned liquid multi column damper is a Bidirectional TLCD presented in Rozas (2016), with the geometry configuration presented in Figure 6.

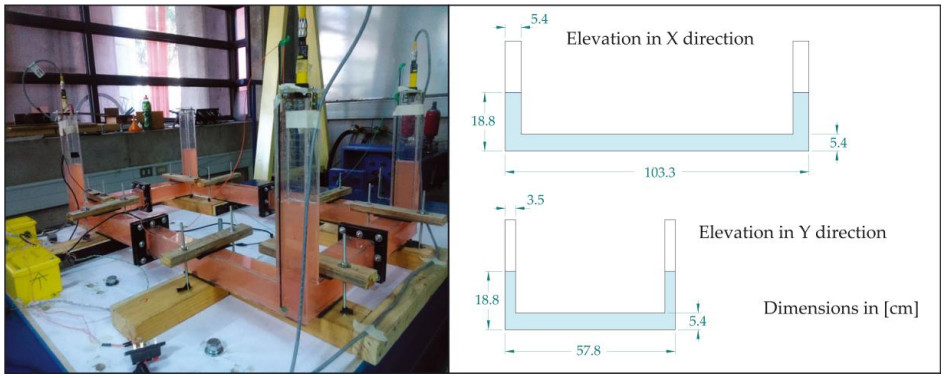

Figure 6. Bidirectional TLCD main dimensions (Rozas 2016).

As in a bidirectional study subject, the natural frequencies are now evaluated in both X and Y directions. The resultant modes and natural frequencies (Table 4) were then compared with the analytic solution and experimental data (Rozas et al. 2016).

Table 4. Convergence results for natural modes of vibration and frequencies of the BTLCD.

Direction	Analytic	Experimental	Present Study	Error analytic	Error experimental (%)
X	0,618	0,617	0,632	2,26%	2,48%
Y	0,857	0,861	0,885	3,27%	2,79%

The presents results (Table 4) show reasonable concordance with both analytic and experimental results with divergences lower than 3,5% to the analytical solution and under 2,8% to the experimental results. Figure 7 show the first two modal shapes of TMLCD in directions X and Y, respectively.

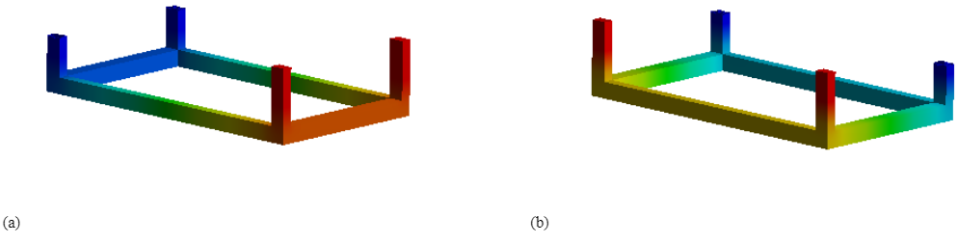

(a) (b)

Figure 7. Resonance modes of the BTLCD (a) First mode, in X direction ($\omega_1 = 0.632\ Hz$), (b) Second mode, in Y direction ($\omega_2 = 0.885\ Hz$).

Coupling the acoustic body to the damper shell leads to some increase in the mass of the system and the addition of flexible walls, which influences the natural frequency of the set, from 0,632 and 0,885 Hz to 0,634 and 0,888 Hz leading to divergences with the experimental results of 2,75 and 3,14% in the X and Y directions respectively.

Continuing the work, the harmonic analysis consists coupling the bidirectional set to a spring mass system of the same natural frequency (K= 15868 N/m, mass = 992,9 kg) to evaluate the influence of the damper on the oscillation of this system in the X direction.

Figure 8 shows the system coupled to the structure and its boundary conditions

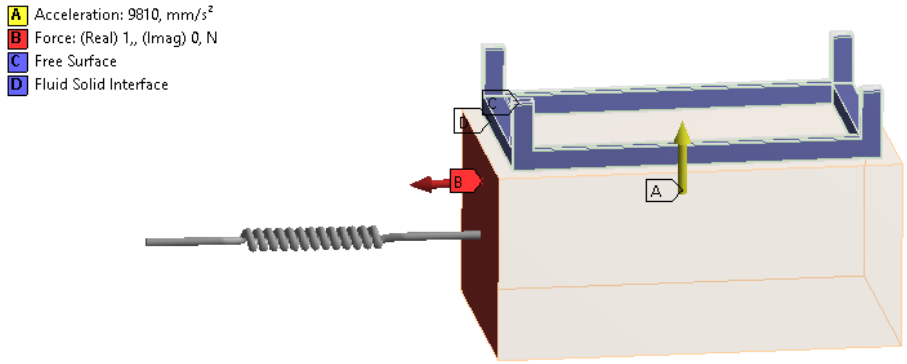

Figure 8. Coupled system and boundary conditions.

The harmonic analysis was performed discretizing the acoustic body with FLUID221 elements, which allow fluid-structure interactions, applied in the contact regions between the fluid and damper shell, the force applied to the spring mass system was 1N applied on the left face of the mass and the frequency response function was collected at the extreme right corner of the mass block.

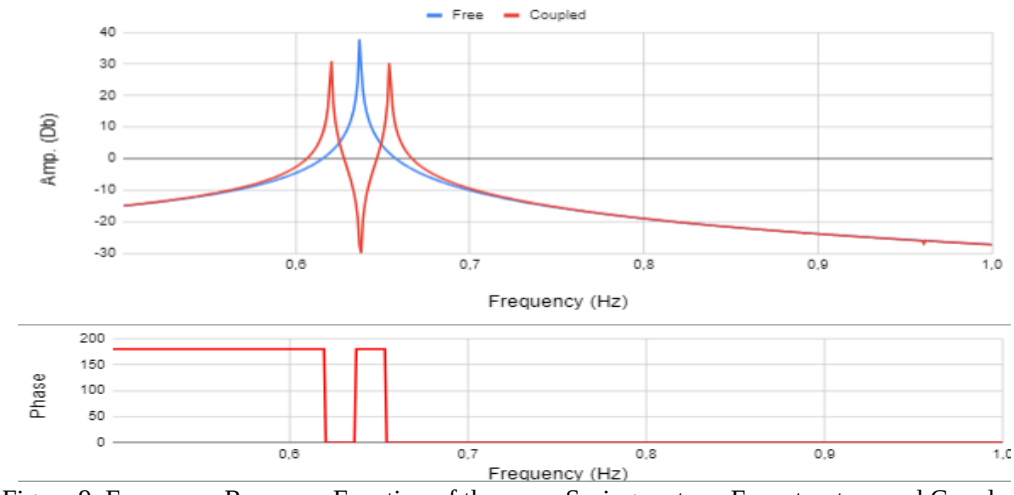

Figure 9. Frequency Response Function of the mass-Spring system, Free structure and Coupled.

The coupling effects of the device presented by Figure 9, demonstrate accordance with the theory of mechanical vibrations showing a reduction of amplitude of 44,88% or 6,96 Db in the coupled system to the force of 1N applied at the system, verifying the efficiency of this type of device.

6. CONCLUSION

This study was comparing the ANSYS Workbench simulation of fluid-structure sloshing problems, such as rectangular container, TLCD and TMLCD, with literature and analytical solution. The fluid domain is discretized by isoparametric elements (FLUID220 and FLUID221).

Three problems were presented: (a) a rectangular water tank, (b) a U-shaped tube damper (TLCD) and (c) a multiple column liquid damper (TMLCD). For first example, the numerical solutions present acceptable relative error (inferior to 0.2% relative error) when compared to analytical solutions.

For the second case, the TLCD example, the numerical results were validated using experimental results and previous numerical studies, presenting acceptable errors (6% relative error).

For the last one, the results were compared to the analytic solution and previous works returning a relative error of 3,14%, relative to experimental results from Rozas, when coupled to the device's shell, and the coupled harmonic analysis presented satisfactory results, a reduction of 6,96 Db from the main to the residual peaks, proving the efficiency of this kind of device in dampening low frequencies.

The present cases comparations show reasonable agreement with literature and analytical solution. Some numerical sources of errors must be explored par report to this present exploratory study. More tridimensional example must be explored and coupled examples with non-linear Navier-stokes fluid equations must be explored and evaluated in fatigue response.

7. ACKNOWLEDGEMENTS

The present study was financed by Brazilian National Conseil of Research and Development (Conselho Nacional de Pesquisa e Desenvolvimento - CNPq) with partnership with University of Brasilia by Edictal 2022/2023 PROIC/UnB-CNPq. The authors acknowledge to CNPq and UnB by resources that make possible the present work.

8. REFERENCES

Alkmim, M. H., Adriano T. Fabro, and Marcus V. G. de Morais. 2018. "Optimization of a Tuned Liquid Column Damper Subject to an Arbitrary Stochastic Wind." *Journal of the Brazilian Society of Mechanical Sciences and Engineering* 40(11):1–11. doi: 10.1007/s40430-018-1471-3.

Colwell, Shane, and Biswajit Basu. 2009. "Tuned Liquid Column Dampers in Offshore Wind Turbines for Structural Control." *Engineering Structures* 31(2):358–68. doi: 10.1016/j.engstruct.2008.09.001.

Martins, Juliano Ferreira, Marcus V. G. de Morais, and Suzana Moreira Avila. 2019. "Experimental Study of Equivalente 1DoF Main Structure Coupled to TLCD: Validation of Optimum Parameter Obtained by Parametric Optimization." Pp. 1–4 in *25th ABCM International Congress of Mechanical Engineering*, edited by ABCM. Uberlândia: UFU.

Rozas, Luis, Ruben L. Boroschek, Aldo Tamburrino, and Matías Rojas. 2016. "A Bidirectional Tuned Liquid Column Damper for Reducing the Seismic Response of Buildings." *Structural Control and Health Monitoring* 23(4):621–40. doi: 10.1002/stc.1784.

Sakai, F., S. Takaeda, and T. Tamaki. 1989. "Tuned Liquid Column Damper-New Type Device for Suppression of Building Vibrations." Pp. 926–31 in: *Proceedings of international conference on highrise buildings.* Nanjing.

da Silva, Agnaldo Antônio Moreira T., and Marcus Vinicius Girão de Morais. 2018. "FE Sloshing Modelling in Bidimensional Cavity Using Wave Equation" edited by N. Maia and Z. Dimitrovová. *MATEC Web of Conferences* 211:07001. doi: 10.1051/matecconf/201821107001.

Yalla, Swaroop K., and Ahsan Kareem. 2000. "Optimum Absorber Parameters for Tuned Liquid Column Dampers." *Journal of Structural Engineering New York, N.Y.* 126(8):906–15. doi: 10.1061/(ASCE)0733-9445(2000)126:8(906).

9. RESPONSIBILITY NOTICE

The author(s) is (are) the only responsible for the printed material included in this paper.